Micro- and nanostructuring of freestanding, biodegradable, thin sheets of chitosan via soft lithography

Javier G. Fernandez,[1] Christopher A. Mills,[1] Elena Martinez,[1] Maria J. Lopez-Bosque,[1] Xavier Sisquella,[1] Abdelhamid Errachid,[1,2] Josep Samitier[1,2]

[1]*Laboratory of Nanobioengineering (IBEC), Barcelona Science Park, c/Josep Samitier 1-5, 08028 Barcelona, Spain*
[2]*Department of Electronics, University of Barcelona, c/Martí i Franquès 1, 08028 Barcelona, Spain*

Received 27 March 2006; revised 22 February 2007; accepted 5 June 2007
Published online 9 August 2007 in Wiley InterScience (www.interscience.wiley.com). DOI: 10.1002/jbm.a.31561

Abstract: A technique for imparting micro- and nanostructured topography into the surface of freestanding thin sheets of chitosan is described. Both micro- and nanometric surface structures have been produced using soft lithography. The soft lithography method, based on solvent evaporation, has allowed structures ~60 nm tall and ~500 × 500 nm^2 to be produced on freestanding ~0.5 mm thick sheets of the polymer when cured at 293 K, and structures ~400 nm tall and 5 × 5 μm^2 to be produced when cured at 283 K. Nonstructured chitosan thin sheets (~200 μm thick) show excellent optical transmission properties in the visible portion of the electromagnetic spectrum. The structured sheets can be used for applications where optical microscopic analysis is required, such as cell interaction experiments and tissue engineering. © 2007 Wiley Periodicals, Inc. J Biomed Mater Res 85A: 242–247, 2008

Key words: chitin/chitosan; microstructure; nanotopography; polymerization; soft lithography

INTRODUCTION

Biopolymers are increasingly being studied in relation to their interactions with cell cultures for applications such as tissue engineering[1] and biomedical implants.[2] In such applications, it is probable that the surface topography of the biopolymer plays an important role in the well-being of the growing cells.[3–7] To this end, polymers with properties suitable for biomedical applications have been investigated with respect to the ability to impart ordered structure into their surfaces.[8–11]

Chitin, a high molecular weight nitrogenous polysaccharide, is the second most abundant natural biopolymer, and is commonly found in the shells of marine crustaceans, the exoskeleton of insects, and the cell walls of fungi. Chitosan is a deacetylated derivative of chitin (Fig. 1), and is a linear polysaccharide, composed of glucosamine and *N*-acetyl glucosamine units covalently linked via β(1–4) bonds. The glucosamine/*N*-acetyl glucosamine ratio is normally referred to as the degree of deacetylation.[12] The high abundance of chitin, and hence chitosan, makes chitosan a promising material for use in biomedical applications where biopolymers are necessary.

Chitosan has a number of properties that make it attractive for use in biomedical applications. It has intrinsic antibacterial activity as its cationic amino group associates with anions on the bacterial cell wall, which accelerate bacterial mortality.[13] This cationic nature also means that chitosan interacts electrostatically with anionic glycosaminoglycans (GAG), proteoglycans, and other negatively charged molecules. These interactions lead to some interesting chitosan properties.[14] For example, a large number of cytokines/growth factors are linked to GAG (mostly with heparin and heparin sulphanate) and, therefore, a surface or scaffold containing the chitosan-GAG complex may retain and concentrate growth factors secreted by colonizing cells. Other characteristics of chitosan are the stimulatory effect of its oligosaccharides on macrophages, and the chemoatractivity of neurophils of chitosan both *in vivo* and *in vitro*.

Depending on the source and preparation procedure, the molecular weight of chitosan may vary from 300 to ~1000 kDa with a degree of deacetylation from 30 to 95%. In its crystalline form chitosan is normally insoluble in aqueous solutions above

Correspondence to: C. A. Mills; e-mail: cmills@pcb.ub.es
Contract grant sponsor: European Community (CellPROM project); contract grant number: NMP4-CT-2004-500039
Contract grant sponsor: Spanish Ministry for Science and Education (FPU and Ramon y Cajal grants)

© 2007 Wiley Periodicals, Inc.

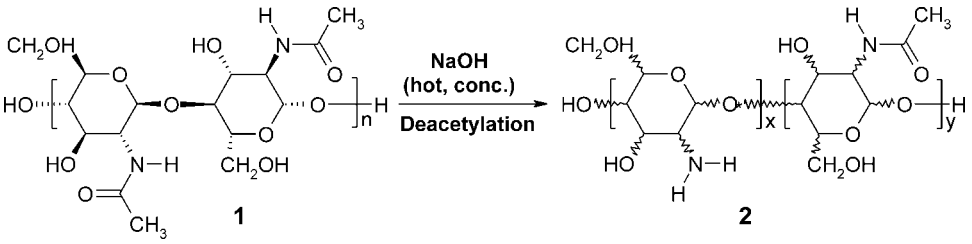

Figure 1. Reaction scheme showing the production of Chitosan **2** from Chitin **1**. The ratio of the glucosamine (x) and the *N*-acetyl glucosamine (y) in the chitosan is referred to as the degree of deacetylation.

pH 7; however, in dilute acids (pH < 6) the protonated free amino groups on glucosamine help to solubilize the polymer, and hence facilitate processing.[15,16]

Chitosan is degraded *in vivo* through the hydrolysis of acetylated residues by lysozyme enzymes.[17,18] Other proteolytic enzymes also degrade chitosan, with the rate of polymer degradation being inversely related to the degree of deacetylation. This makes it an excellent candidate for applications where biodegradable polymers are required. For example, possible chitosan matrix preparations include gels, sponges, fibres, beads, or porous compositions.[19–23] However, nature has demonstrated that it is possible to form nanometric structures from chitosan, in the form of cicada wings.[24] Planar sheets of chitosan containing ordered micro- or nanostructures may be useful in such applications as tissue culturing and cell interaction experiments. For employment as a substrate for cell culturing, the structured chitosan film can be further treated with sodium hydroxide (NaOH) in order to neutralize any possible acid residues and to complete surface deacetylation.[25] Here we present the ordered topological structuring of chitosan polymer at micro- and nanoscales using soft lithography techniques.

MATERIALS AND METHODS

Chitosan solution preparation

Medium molecular weight chitosan (75–85% deacetylated, 200–800 cps viscosity), derived from crab shell, was purchased from Aldrich (Sigma-Aldrich Chemical, USA). A 2% (w/v) polymer solution was produced by dissolving the chitosan in dilute glacial acetic acid (1% v/v). The chitosan polymer solution was subjected to ultrasonic agitation and heated at 35°C to aid solvation. After ~90 min the resultant solution was a highly viscous, transparent fluid with a yellow color.

However, possibly due to the source of the chitosan (from crab shells), the polymer solution was full of submillimetre sized particles, which could not be removed via filtration because of their high concentration, and were not dissolved with further ultrasonic/heat treatments. To remove these particles, the chitosan solution was placed in a centrifuge at 20,000 rpm for 10 min. The particle free polymer solution could then be decanted for use in the structuring experiments.

Thin film deposition

To ensure the processability of the chitosan solution with respect the production of thin polymer films, it was spun down onto glass substrates (WS-400A Laurel Technologies Corp., USA) (Fig. 2). The polymer solution was spread on the surface of the substrate (~0.2 mL cm^{-2}), and a dispensing spin was performed at 500 rpm for 10 s, to ensure the substrate is evenly covered with polymer, before accelerating to the final spin speed for 45 s. A 3 min post-deposition soft bake at 65°C was completed to cure the polymer film.

Mould fabrication

Moulds containing structures, which are the negative of those required in the polymer, were prepared using previously described methods.[26] Microstructured moulds were prepared using deep reactive ion etching (RIE), whereas nanostructured moulds were produced using focussed ion beam (FIB) milling techniques. In each case, the material

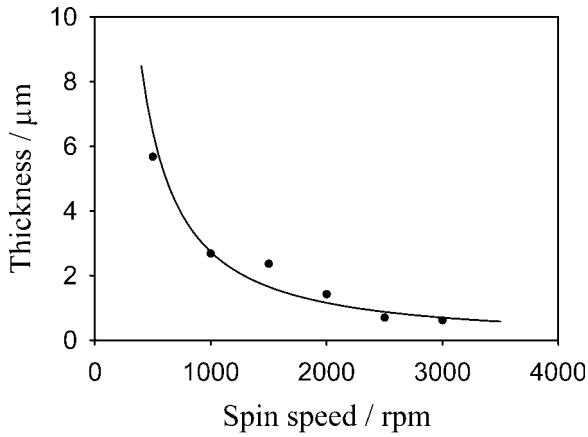

Figure 2. Spin curve data (circles) showing the thickness of chitosan films deposited onto glass substrates from a 2% (w/v) chitosan solution in acetic acid. The data are compared to a theoretical curve (solid line) describing the thickness variation of thin films spun down onto substrates.[28]

used for the moulds was silicon-based and the surface to come in contact with the polymer was silicon nitride. The moulds fabricated are arrays of holes of 5×5 μm^2 and 400 nm deep (microstructured) and $\sim 500 \times 500$ nm^2 and 70 nm deep (nanostructured).

The mould was cleaned via a solvent rinse (acetone, ethanol, and water) before drying under nitrogen. A final clean in an oxygen plasma cleaner was undertaken for 20 min. The antiadhesion property of the silicon nitride was enhanced by depositing a silane-based antiadhesion coating on the surface prior to use.[27]

Chitosan micro- and nanostructuring

Micro- and nanostructure replication in chitosan has been attempted via soft lithography from a 2% (w/v) solution of chitosan. The soft lithography is carried out by pouring polymer solution onto the mould and allowing the solvent to evaporate in a fume hood. After the evaporation of the acidic solvent, a hard, ~0.5-mm thick layer of chitosan forms on the mould surface containing negative replicas of the structures in the mould. The chitosan film is then manually removed from the mould with the help of tweezers, and the freestanding thin polymer sheet deposited on a glass substrate to aid handling. While the chitosan thin sheet replica is mechanically robust (i.e., it does not break or rip easily), its thinness means it has a tendency to bend, causing irreversible folds to appear in the polymer surface.

Initial attempts using a well-ventilated oven to assist in evaporating the solvent had the result of producing unwanted gas bubbles in the chitosan sheet. These gas bubbles are possibly formed by trapped solvent gasses, due to the increased rate at which the chitosan solidifies.

Characterization

The structured, thin chitosan sheets have been topologically characterized using a variety of methods depending on the dimensions of the structures produced in the surface. For the microstructured polymers, the surface was examined using a microscope, to confirm the production of the structures, and then white light interferometry (Wyko NT1100 Optical interferometer, Veeco Instruments, USA), in vertical scanning interferometry mode, was used to produce a three-dimensional rendering of the surface from which structure dimensions could be measured. The interferometric technique is ideal for imaging these surfaces as a large area of the surface (70×70 μm^2) can be imaged with a high vertical resolution (~2 nm). The imaging time is in the order of 30 s, which allows rapid, highly accurate measurements of a number of micrometric posts (~40) simultaneously.

For the nanostructures, the surface was first examined using scanning electron microscopy (SEM, Strata DB35 dual beam FIB/SEM, FEI company, USA) to confirm the presence of the structures, before atomic force microscopy (AFM, MFP-3D AFM, Asylum Research, USA) was used to produce a three-dimensional image from which structural dimensions could be measured. AFM was carried out in contact mode, in ambient conditions, using a silicon nitride AFM probe with a force constant of 80 pN nm^{-1} (OMCL TR400PSA-2, Atomic Force F&E GmbH, Germany). Finally, the optical transparency of a ~200 μm thick, freestanding film of the chitosan was tested using UV-visible spectroscopy (UV-2501PC UV-Visible Spectrometer, Shimadzu Corp., Japan).

The thickness of the polymer layer spun onto glass is measured using a profilometer (Dektak Surface Profiler, Veeco Instruments, USA). A section of the chitosan is removed using a sharp blade and the step height of the polymer to the glass is measured.

RESULTS AND DISCUSSION

The successful production of chitosan thin films, deposited on glass, with thicknesses ranging from 6.5 to 0.7 μm (Fig. 2) shows that the chitosan prepared here is suitable for thin film processing using existing techniques. Indeed, the spin curve data in Figure 2 has been favorably compared ($R^2 = 0.9292$) with a theoretical curve describing the variation in thickness of thin films spun down on to substrates.[28] The theory describes an equation for the thickness of the final polymer thin film, of the form $y = b \times x^{-a}$, where y is the film thickness, x is the spin speed (rpm), and a and b are empirical characteristics of the polymer: in the case of chitosan, $a = 1.24$ and $b = 14{,}326$. The chitosan, when spun down in this way, produces a transparent polymer film with micrometer or sub-micrometer thickness on the surface of the glass. These films are eminently useful when microscopic apparatus is to be used for optical characterization of cellular interactions with the chitosan, for example. However, a method that will allow the interactions of cells with structured chitosan surfaces is now of interest, considering that there is evidence that polymer topography has an effect on cells cultured on the polymer surface.[29–33]

Initially, nanoembossing of structures in to the surface of chitosan thin films spun down onto glass substrates, was attempted using a nanoimprinter (Obducat 2.5 inch nanoimprinter, Obducat AB, Sweden). Several embossing conditions were attempted at temperatures ranging from 80 to 130°C and at pressures from 3×10^6 to 5×10^6 Nm^{-2}, all of them performed for an embossing time of 600 s. Unfortunately all the embossing attempts were unsuccessful because no structures, or even regular deformations, were formed on the surface of the polymer. This may be due to the fact that after spinning down the chitosan, most of the solvent had been evaporated and the polymer was extremely rigid. We conclude that the chitosan in this state (i.e., in a dried thin film) is not suitable for structuring by nanoembossing because it is not thermoplastic enough, and

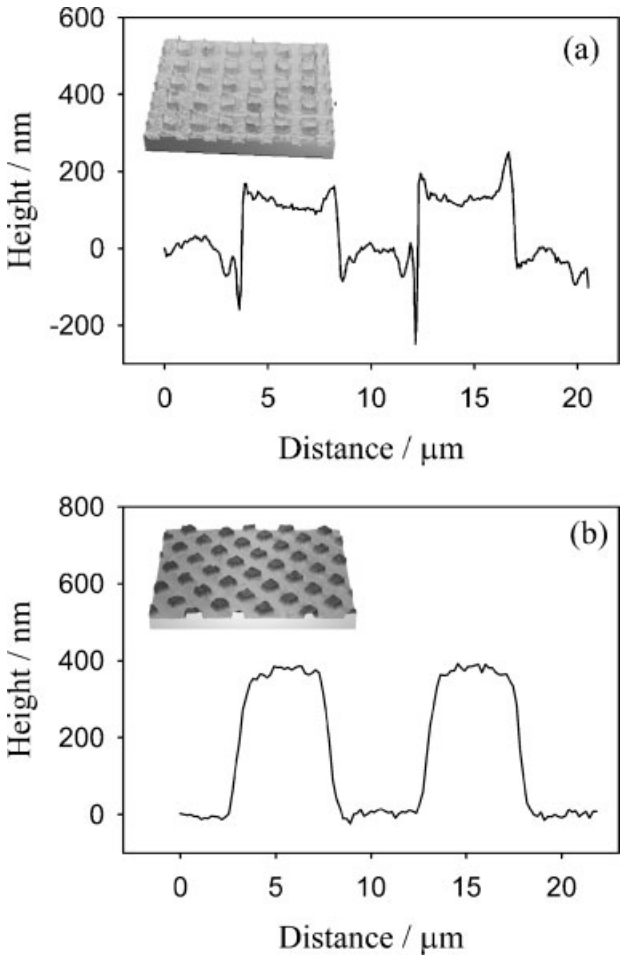

Figure 3. Sectional profiles of microstructures produced on a freestanding, ~500 μm thick chitosan sheet via soft lithography. The sectional profiles show the 5 × 5 μm^2 structures, with a 10 μm period, produced in the surface of the polymer when cured at (a) 293 K and (b) 283 K. The sectional profiles are taken from white light interferometer images [scan area = 58 × 45 μm^2] shown inset.

shows no sign of having the capacity to undergo a glass transition process to form a softened state suitable for nanoimprinting. Therefore, a more suitable structuring technique for polymer in solution is required, and hence the use of soft lithography.

Both micro- and nanostructures have been fabricated in the surface of freestanding, thin chitosan sheets via the soft lithography technique described. Although the microstructures (Fig. 3) have replicated in the surface of the polymer after curing at 293 K, their height corresponds to only ~50% of the depth of the mould used in the soft lithography (400 nm). The concave shape of the tops of the posts in the chitosan replicas are also an indication of incomplete replication,[34] and is possibly due to the chitosan curing before it has chance to displace the air in the cavities and reach the bottom of the mould structures.

To confirm this hypothesis the chitosan was cured at low temperature (283 K) to reduce the evaporation rate of the solvent. This increases the capacity of the air in the cavities to dissolve into the polymer solution and allows the polymer to displace it in the mould cavities. The replicated polymer surface

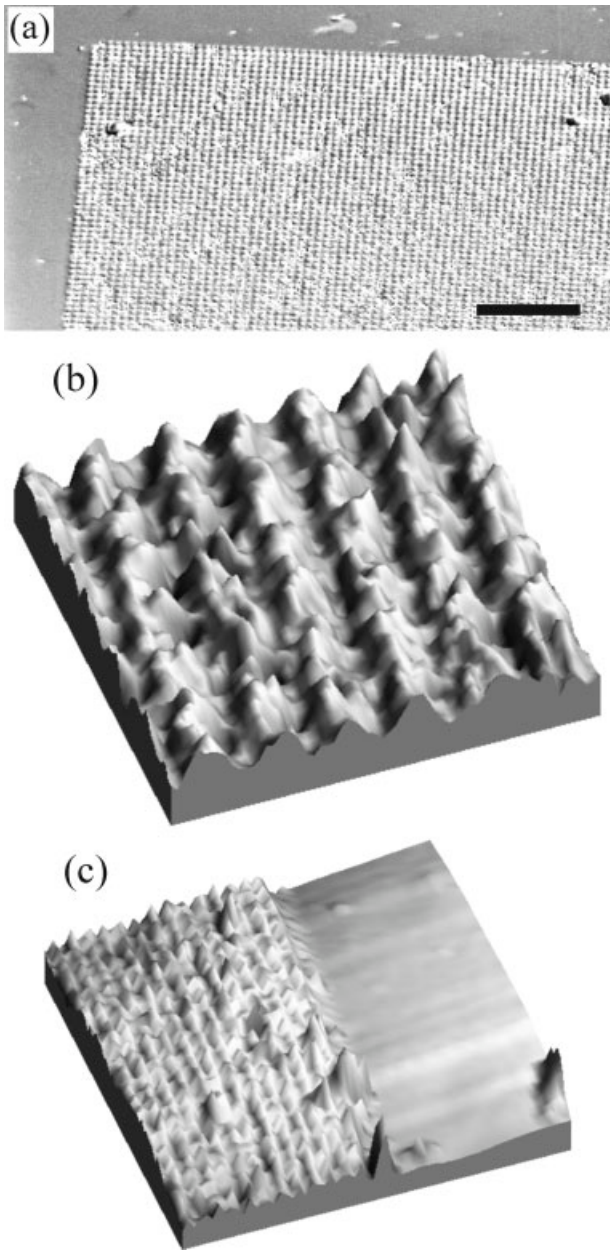

Figure 4. (a) SEM image [bar = 10 μm] of nanostructures reproduced on a freestanding, ~500 μm thick chitosan sheet via soft lithography. (b) AFM image of the nanostructures which are ~60 nm tall, ~500 × 500 nm^2 with a 1 μm period [scan area = 5 × 5 μm^2]. (c) AFM image of the edge of the nanostructured area [scan area = 20 × 20 μm^2]. Average roughness measurements: R_a (nonstructured area) = 9.6 nm, R_a (nanostructured area) = 46.7 nm [measurement area in each case = 4.7 × 4.7 μm^2].

shows a high fidelity to the mould. However, a major drawback to this technique is that the curing process now takes almost five times longer (10 days) at this temperature. The temperature of the environment during curing is therefore a variable parameter depending of the needs of the application, that is, depending on the requirement for speed or accuracy of replication.

We have attempted to use both silicon and poly(-dimethyl siloxane) (PDMS, Slygard 184, Microchem Corp., USA) moulds from which to impart the structures in the surface of the polymer. The PDMS moulds, however, have a poor affinity with polymerized chitosan, causing spontaneous separation of the mould and the replica during polymerization. In comparison, contact between the polymer and the mould is continuous during the whole evaporation process when using silicon-based moulds. However, the PDMS does not have a bad affinity for the chitosan solution in acetic acid, suggesting that the chitosan solution could be used in PDMS based microfluidics if required.

Nanostructures with dimensions of 60 nm tall, $\sim 500 \times 500$ nm^2 at the base, and 1 μm period have been fabricated using a silicon mould produced via FIB (Fig. 4). In this case, the height of the nanostructures corresponds to ~73% of the depth of the holes fabricated in the mould. The nanostructures are, however, somewhat irregular, possibly due to some adherence of the polymer to the mould upon demoulding. Even so, the nanostructures cover the entire 1 mm^2 nanostructured area defined in the mould.

A comparison of the nanostructured area with that of the embossed but nonstructured areas of the chitosan [Fig. 4(c)] reveals that the nanostructured area has a roughness ~3 times greater than that of the nonstructured area. Roughness measurements measured in 4.7×4.7 μm^2 areas give average roughness (R_a) values of 9.6 nm for the nonstructured area and 46.7 nm for the nanostructured area, respectively. This increase in the roughness of the surface, allied with the size of the nanostructures, suggests that these structured chitosan surfaces will be "felt" by cells cultured on the surface,[35,36] and will have uses in cell-surface interaction studies and tissue engineering.

Optical transmittance spectra, recorded over the visible range of the electromagnetic spectrum, of a ~200 μm thick freestanding sheet of nonstructured chitosan is given in Figure 5. The polymer sheets have excellent optical transparency (~90%) in this region. The addition of the micro-/nanostructures will reduce the transparency somewhat, but they are still expected to be extremely useful for optical microscopy studies where cell-surface interactions are required.

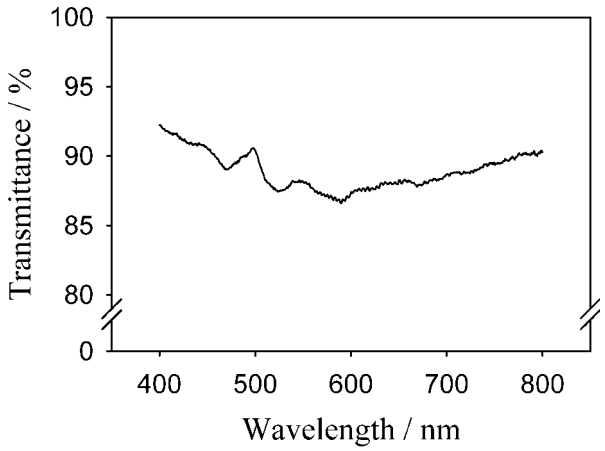

Figure 5. Optical transmittance spectra of a ~200 μm thick freestanding film of chitosan. The spectrum is recorded over the visible range of the electromagnetic spectrum.

CONCLUSION

Micro- and nanostructures have been produced in freestanding, thin films of chitosan using a soft lithography technique, and the quality of the replicas has been studied with respect to the curing temperature and time. The nanostructures have been produced in the surface with dimensions that have previously been shown to affect cell culture.[35,36] The optical transparency of the chitosan thin films means that they can be utilized in applications requiring optical microscopy techniques, such as those commonly used in biological laboratories. Such surfaces will be useful for cell-surface studies or applications involving tissue engineering. The solution processability of the chitosan is also described by the production of a spin curve for deposition of the polymer onto glass substrates, confirming chitosan's applicability for the production of thin films. Further development will be undertaken, focusing on the preparation of the chitosan solution, to produce a polymer that is more able to fabricate micro- and nanostructures to their full height in more robust thin sheets, and for possible use in techniques such as polymer embossing. This may be achieved by preparing a polymer with a more amorphous character for example.

The authors thank Drs. J. Bausells and G. Villanueva at the Centro Nacional de Microelectronica (Barcelona) for supplying the microstructured moulds used here.

References

1. Di Martino A, Sittinger M, Risbud MV. Chitosan: A versatile biopolymer for orthopaedic tissue-engineering. Biomaterials 2005;26:5983–5990.

2. Mano JF, Sousa RA, Boesel LF, Neves NM, Reis RL. Bioinert, biodegradable and injectable polymeric matrix composites for hard tissue replacement: State of the art and recent developments. Compos Sci Technol 2004;64:789–817.
3. Tan WJ, Teo GP, Liao K, Leong KW, Mao H-Q, Chan V. Adhesion contact dynamics of primary hepatocytes on poly (ethylene terephthalate) surface. Biomaterials 2005;26:891–898.
4. Vance RJ, Miller DC, Thapa A, Haberstroh KM, Webster TJ. Decreased fibroblast cell density on chemically degraded poly-lactic-*co*-glycolic acid, polyurethane, and polycaprolactone. Biomaterials 2004;25:2095–2103.
5. Wang YC, Ho C-C. Micropattering of proteins and mammalian cells on biomaterials. FASEB J 2004;18:525–527.
6. Ruoslahti E, Reed JC. Anchorage dependence, integrins, and apoptosis. Cell 1994;77:477–478.
7. Curtis ASG, Casey B, Gallagher JO, Pasqui D, Wood MA, Wilkinson CDW. Substratum nanotopography and the adhesion of biological cells. Are symmetry or regularity of nanotopography important? Biophys Chem 2001;94:275–283.
8. Mills CA, Navarro M, Engel E, Martinez E, Ginebra MP, Planell J, Errachid A, Samitier J. Transparent micro- and nanopatterned poly(lactic acid) for biomedical applications. J Biomed Mater Res A 2006;76:781–787.
9. Kim HJ, Kim U-J, Vunjak-Novakovic G, Min B-H, Kaplan DL. Influence of macroporous protein scaffolds on bone tissue engineering from bone marrow stem cells. Biomaterials 2005;26:4442–4452.
10. Agrawal CM, Ray RB. Biodegradable polymeric scaffolds for musculoskeletal tissue engineering. J Biomed Mater Res 2001; 55:141–150.
11. Drury JL, Mooney DJ. Hydrogels for tissue engineering: Scaffold design variables and applications. Biomaterials 2003;24: 4337–4351.
12. Khan TA, Peh KK, Ch'ng HS. Reporting degree of deacetylation values of chitosan: The influence analytical methods. J Pharm Pharm Sci 2002;5:205–212.
13. Aimin C, Chunlin H, Juliang B, Tinyin Z, Zhichao D. Antibiotic loaded chitosan bar. An in vitro, in vivo study of a possible treatment for osteomyelitis. Clin Orthop Relat Res 1999;366:239–247.
14. Madihally SV, Matthew HWT. Porous chitosan scaffolds for tissue engineering. Biomaterials 1999;20:1133–1142.
15. Rinaudo M, Pavlov G, Desbrieres J. Solubilization of chitosan in strong acid medium. Int J Polym Anal Char 1999;5:267–276.
16. Sorlier P, Denuziere A, Viton C, Domard A. Relation between the degree of acetylation and the electrostatic properties of chitin and chitosan. Biomacromolecules 2001;2:765–772.
17. Nordtveit RJ, Vårum KM, Smidsrød O. Degradation of fully water-soluble, partially *N*-acetylated chitosans with lysozyme. Carbohydr Polym 1994;23:253–260.
18. Nordtveit RJ, Vårum KM, Smidsrød O. Degradation of partially *N*-acetylated chitosans with hen egg white and human lysozyme. Carbohydr Polym 1996;29:163–167.
19. Bhattarai N, Edmondson D, Veiseh O, Matsen FA, Zhang M. Electrospun chitosan-based nanofibers and their cellular compatibility. Biomaterials 2005;26:6176–6184.
20. Ma L, Gao C, Mao Z, Zhou J, Shen J, Hu X, Han C. Collagen/chitosan porous scaffolds with improved biostability for skin tissue engineering. Biomaterials 2003;24:4833–4841.
21. Mi F-L, Shyu S-S, Wu Y-B, Lee S-T, Shyong J-Y, Huang R-N. Fabrication and characterization of a sponge-like asymmetric chitosan membrane as a wound dressing. Biomaterials 2001; 22:165–173.
22. Lai HL, Abu'Khalil A, Craig DQM. The preparation and characterisation of drug-loaded alginate and chitosan sponges. Int J Pharm 2003;251:175–181.
23. Chen X-G, Liu C-S, Liu C-G, Meng X-H, Lee CM, Park H-J. Preparation and biocompatibility of chitosan microcarriers as biomaterial. Biochem Eng J 2006;27:269–274.
24. Stoddart PR, Dadusch PJ, Boyce TM, Erasmus RM, Comins JD. Optical properties of chitin: Surface-enhanced Raman scattering substrates based on antireflection structures on cicada wings. Nanotechnology 2006;17:680–686.
25. Tolaimate A, Desbrieres J, Rhazi M, Alagui A. Contribution to the preparation of chitins and chitosans with controlled physico-chemical properties. Polymer 2003;44:7939–7952.
26. Mills CA, Martinez E, Bessueille F, Villanueva G, Bausells J, Samitier J, Errachid A. Production of structures for microfluidics using polymer imprint techniques. Microelectron Eng C 2005;78/79:695–700.
27. Bessueille F, Dugas V, Cloarec JP, Vikulov V, Cabrera M, Souteyrand E, Martin JR. Assessment of porous silicon substrate for well-characterised sensitive DNA chip implement. Biosensors Bioelectron 2005;21:908–916.
28. Malangone R, Needham CD. An investigation of the thickness variation of spun-on thin films commonly associated with the semiconductor industry. J Electrochem Soc 1982;129: 2881–2883.
29. Anselme K. Osteoblast adhesion on biomaterials. Biomaterials 2000;21:667–681.
30. Martin JY, Schwartz Z, Hummert TW, Schraub DM Simpson J, Lankford J, Dean DD, Cochran DL, Boyan BD. Effect of titanium surface roughness on proliferation, differentiation, and protein synthesis of human osteoblast-like cells (MG63). J Biomed Mater Res 1995;29:389–401.
31. Lincks J, Boyan BD, Blanchard CR, Lohmann CH, Liu Y, Cochran DL, Dean DD, Schwartz Z. Response of MG63 osteoblast-like cells to titanium and titanium alloy is dependent on surface roughness and composition. Biomaterials 1998;19:2219–2232.
32. Matsuzaka K, Walboomers XF, de Ruijter JE, Jansen JA. The effect of poly-L-lactic acid with parallel surface micro groove on osteoblast-like cells in vitro. Biomaterials 1999;20:1293–1301.
33. Matsuzaka K, Walboomers XF, Yoshinari M, Inoue T, Jansen JA. The attachment and growth behaviour of osteoblast-like cells on microtextured surfaces. Biomaterials 2003;24:2711–2719.
34. Heyderman LJ, Schift H, David C, Gobrecht J, Schweizer T. Flow behaviour of thin polymer films used for hot embossing lithography. Microelectron Eng 2000;54:229–245.
35. Wilkinson CDW, Riehle M, Wood M, Gallagher J, Curtis ASG. The use of materials patterned on a nano- and micrometric scale in cellular engineering. Mater Sci Eng C 2002; 19:263–269.
36. Curtis A, Wilkinson C. Topographical control of cells. Biomaterials 1997;18:1573–1583.